doi: 10.17116/engoftalma20171331-4

Comparative analysis of the value of information provided by anterior segment optical coherence tomography and in vivo confocal microscopy for identifying the palisades of Vogt in normal limbus

N.P. PASHTAEV, N.A. POZDEYEVA, A.A. VOSKRESENSKAYA, B.V. GAGLOEV, A.A. SHIPUNOV

Cheboksary branch of S. Fyodorov Eye Microsurgery Federal State Institution, pr. Tractorostroiteley 10, Cheboksary, Russian Federation, 428028

Aim — to conduct a comparative analysis of the value of information provided by anterior segment optical coherence tomography (AS-OCT) and in vivo confocal microscopy (IVCM) for identifying the palisades of Vogt (POV) in normal limbus. **Material and methods.** POV at the superior and inferior limbus were studied in 15 healthy participants (30 eyes) without any anterior segment diseases. Two examination methods were used: AS-OCT En Face imaging (RTVue XR Avanti, 3D Cornea protocol) and IVCM (HRT3). Concordance of the results was then analyzed. **Results.** Structural features of POV were distinguishable by both methods. LSCM was able to visualize POV in superior and inferior limbus of all 15 patients (30 eyes). Within the inferior corneal hemisphere, POV had the appearance of well-differentiated, hyperreflective, double-contoured structures organized in parallel lines at level of basal epithelium. The structure of superior limbus, as judged from LSCM data, varied significantly: "classic" palisades was revealed in only 13 eyes (43%), while in other 17 cases (57%) POV were atypical. On AS-OCT, POV structure was seen in detail in 29 eyes. By comparing the abilities of LSCM and AS-OCT to visualize POV, a strong positive correlation ($r_s = 0.99$, $p<0.05$) was revealed between the results obtained in both the superior and inferior limbus. **Conclusion.** AS-OCT data provide a detailed understanding of POV structure and strongly correlate with LSCM results. Taking into consideration the noninvasiveness, demonstrativeness, repeatability of AS-OCT En Face imaging as well as the high value of provided information, the method can be recommended as an alternative in POV diagnostics.

Keywords: *limbal palisades of Vogt, focal stromal projections, limbal epithelial stem cells, anterior segment optical coherence tomography (AS-OCT), in vivo confocal microscopy (IVCM), limbus.*

Vestnik_Oftalmologii_2017-1_60EN

The limbal palisades of Vogt (POV) were discovered in 1866 by G.J. Henle. But it was A. Vogt who presented a detailed description of this structure in 1921 [1]. A few years later, G. Aurell and T. Kornerup put forward a hypothesis that POV were rudimentary lacrimal glands. But only in 1971 M. Davanger and A. Evensen defined the role of POV in the corneal epithelial regeneration [2]. N. Polisetty et al. demonstrated the presence of limbal stem cells (LSC) in the palisades of Vogt in 1998 [3].

POV are a series of radially oriented fibrovascular ridges located in the thick of the limbus more peripheral to the cornea capillary network. The space between the trabeculae contains corneal epithelium at various stages of differentiation, LSC, melanocytes, Langerhans cells and suppressor T-lymphocytes. The trabeculae contain blood and lymph vessels and subbasal nerve plexus [4–7].

POV are mostly located in the superior and inferior regions of the cornea as opposed to the medial and lateral ones [4, 5, 8]. Their number per unit area of a symmetrical limbus section varies among individuals and may vary depending on the age, surgical interventions and medication use [9–11].

The work of A. Shortt et al. showed that the structures traditionally described as limbal niches (POV) are only part of the limbal architecture. Another component of progenitor structures is represented by focal stromal projections (FSP) located in the apical part of the limbal crypts. Both of the described components contain large amounts of cells small in size, expressing high levels of the LSC markers (ABCG2 and p63α), that have a high nuclear-cytoplasmic ratio as well as a number of other symptoms that make them qualify as stem ones [12]. POV and FSP provides the niche for LSC and play crucial role in maintaining the functioning of the corneal epithelium. They also act as a barrier for the epithelial cells of the conjunctiva and prevent them from migrating to the surface of the cornea. LSC serve as a source with a constant proliferative potential that maintains a pool of corneal epithelial cells. They provide a stable balance between the number of highly differentiated tissue-specific cells and the maintenance of the stem cell depot [6, 7, 13].

Lack of LSC and POV deformations are connected with corneal conjunctivization followed by degenerative

For correspondence:
Voskresenskaya Anna Aleksandrovna — ophthalmologist
e-mail: vsolaris@mail.ru

corneal changes that lead to a substantial vision loss and blindness. Given the lack of direct LSC *in vivo* visualization techniques, studying POV allows one to understand the overall localization and state of progenitor cells.

At the present time, in vivo confocal microscopy (IVCM) is widely used for detecting POV [9, 10, 14]. There is a small number of publications dedicated to POV by anterior segment optical coherence tomography (AS-OCT) [15, 16].

The aim of our work was a comparative analysis of the value of information provided by AS-OCT and IVCM for identifying the POV in healthy individuals.

Material and Methods

15 healthy volunteers (30 eyes) without any anterior eye segment pathology, who did not wear soft contact lenses nor had any history of intraocular surgery, took part in the study. The mean age of subjects was 38.5 ± 13 years (range 23 to 56), 6 men and 9 women.

An AS-OCT of the limbal zone was carried out on an OCT system RTVue XR Avanti (Optovue, USA, software version 2016.1.0.26) with a cornea anterior module long adapter lens, the protocols 3D Cornea and Cornea Cross Line were selected. Scanning zone dimensions for 3D Cornea protocol were 4x4 and 4x6 mm with axial resolution of 5 μm. In all patients, scanning was performed in the superior and inferior limbal sectors within an arc length of 90°. In order to visualize POVs in proper quality a standard scanning layer thickness of 30 micron was used (En Face mode). To look for progenitor structure changes, the depth position of the scan line was adjusted to obtain the sharpest image. The acquired images were analyzed for the presence of POVs with attention to their structural features and visibility. In order to determine the repeatability of the limbus OCT, all the subjects were performed a follow-up study upon in the period from 1 to 7 days. The Cornea Cross Line protocol was used to determine the location of palisades relative to the surface in the superior and inferior limbus.

IVCM was performed on a Heidelberg Retina Tomograph 3 Rostock Corneal Module — HRT3 (Heidelberg Engineering, Germany). The image size was 400x400 μm, the optical section depth was 4 μm. Assessment of POV was conducted in the superior and inferior limbal sectors within 90°. First, operator visualized basal epithelium in the central cornea followed by a shift to the superior or inferior limbus at extreme abduction of the patient's gaze along the vertical meridian. Single operator examined all the patients. LSCM was used as a control and a basic limbal POV detection method.

Correlation analysis of direct (LSCM) and indirect (AS-OCT) imaging of POV was conducted using Spearman›s rank correlation coefficient. The following ranks were assigned for this non-parametric test: 0 — no palisades, 1 — presence of partially modified palisades, 2 — normal appearing palisades.

Results

According to IVCM, in all the 15 subjects (30 eyes) POV were found in the inferior limbus. They were well-differentiable hyperreflective double-contoured structures typically found in the form of parallel lines at the level of the basal epithelium. The length and width of these structures varied considerably, with some related palisades being connected with each other by intersections and others divided at the ends in a dichotomous fashion (**Fig. 1, a–c**). FSP in the form of round or oval formations were located alternating with limbal crypts closer to their apical part (**Fig. 1, c, d**). Different patients had significantly varying numbers of FSP ranging from none to 6–7 projections in sight. Limbal basal cells located along the limbal crypts and FSP in non-pigmented subjects were brighter and had ill-defined margins. They surrounded the structures described as a light halo (**Fig. 1, b, d, h**). In pigmented individuals basal cells had hyperreflective character and were better defined (**Fig. 1, e**) with similar hyperreflective inclusions also occurring in the inter-palisade space (**Fig. 1, f**). The cells between the palisades were characterized by small size, reflective cell borders, dark cytoplasm and nucleus absence. More central from the apical ends of the limbal crypts, dark curvilinear columns or streaks, interrupting the regular mosaic of basal cells, could be seen (**Fig. 1, g**). One non-pigmented subject (30 years old), had on both eyes altered structures of the inferior limbus: limbal crypts were of cellular character appearing as hyperreflective structureless masses in some places, POV was short and uneven in thickness (**Fig. 1, h**).

The junctional zone of the conjunctiva and the cornea epithelium in healthy patients was characterized by inhomogeneous reflectivity and a marked variation in cell size and shape. The cells of the cornea had dark cytoplasm and distinct, bright borders, with the conjunctival cells being smaller in size, less well demarcated and standing out due to high reflectivity (**Fig. 1, i**). The presence of goblet and inflammatory cells on the corneal surface was not observed.

The structure of superior limbus, as judged from LSCM data, varied significantly: "classic" palisades as parallel rows were detected in 13 eyes (43%), while in other 17 cases (57%) POV were atypical (**Fig. 2**). POV on their scleral side exhibited intertwining honeycomb-like structures, terminating with projections of variable length. Atypical "nonclassical" limbal palisades in the superior hemisphere were less structured, more chaotic and variable in shape. Limbal crypts take on circular, honeycomb, hyperreflective appearance; trabeculae were shorter and thinner relative to inferior palisades. FSP occurred in the superior half of the cornea also (**Fig. 2**).

When analyzing the AS-OCT data as per the 3D Cornea protocol in En Face mode the best POV visualization was reached at a scanning depth at the level of the Bowman's membrane or just below it. The bedding range

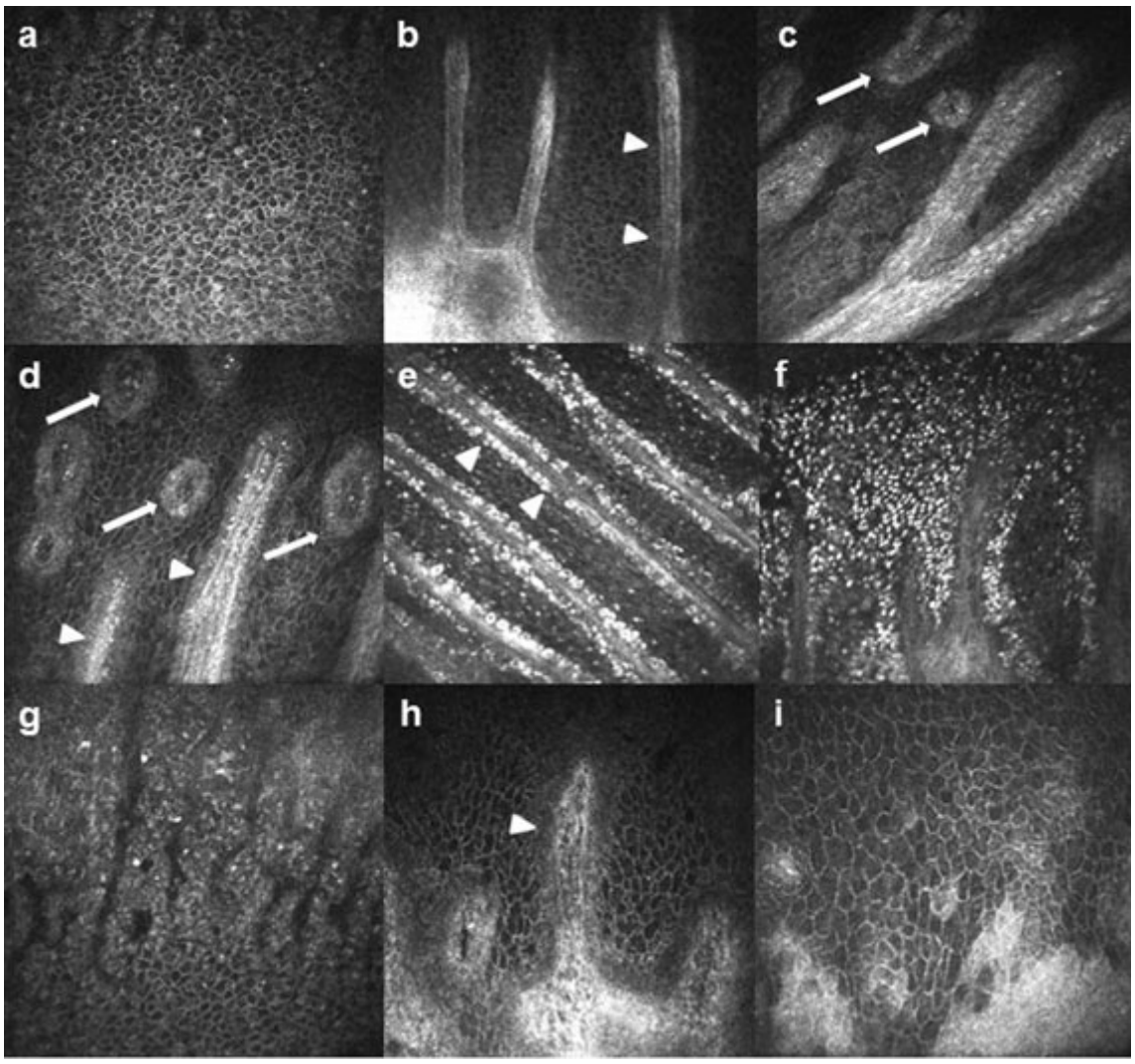

Fig. 1. **IVCM images of the inferior limbus in healthy individuals.**

a — the cells of the basal epithelium with distinct, bright borders, dark cytoplasm and no visible nucleus; b — intact POV connected by a crosspiece, ill-defined limbal basal cells (LBC) are visible along the POV; c — dichotomous division of the apical end of POV, FSP are marked by arrows; d — multiple FSP of oval or round shapes, ill-defined LBC around FSP and POV; e — LBC in pigmented subjects surround POV in the form of hyperreflective contour; f — multiple hyperreflective inclusions in inter-palisade space in pigmented individuals; g — dark "tracks", or "streaks" that interrupt the regular mosaic pattern of basal epithelium; h — short altered POV in a non-pigmented subject; i — normal junction between the corneal and conjunctival cells. In all the images the arrow indicates FSP, and arrow heads indicates LBC.

of limbal progenitor structures varied considerably depending on the thickness of the limbal epithelium. In the inferior limbus, in most cases (28 eyes), POV were identified as ordered elongated hyperreflective trabeculae radially oriented to the cornea (**Fig. 3–5**). The superior limbus had various versions of limbal patterns. In most cases, they were hyperreflective cellular structures generating elongated trabeculae different in length in different subjects (**Fig. 6**). Along with similar patterns, POV were positioned in the form of well-shaped parallel rows or in the form of truncated, short, less contrasting limbal crypts (**Fig. 2**).

The POV localization level was clearly seen on vertical scans performed by Cornea Cross Line protocol. A bed of POV was identified in all patients in the inferior and superior limbus in the form of a typical scleral recess at its corneoscleral transitional zone (**Fig. 7, b**). The horizontal scan showed a visualization of trabeculae in the form of elongated hyperreflective structures repeating the pattern of a typical pile fence (**Fig. 7, a**) especially during studying the inferior limbus.

Repeated limbus studies performed by AS-OCT in all subjects confirmed the repeatability of the previous results (**Fig. 3**).

The features of POV structures were traced and identified according to both research methods (**Fig. 3–6**). An image analysis of limbal progenitor structures according to the data of AS-OCT (3D Cornea protocol) revealed a

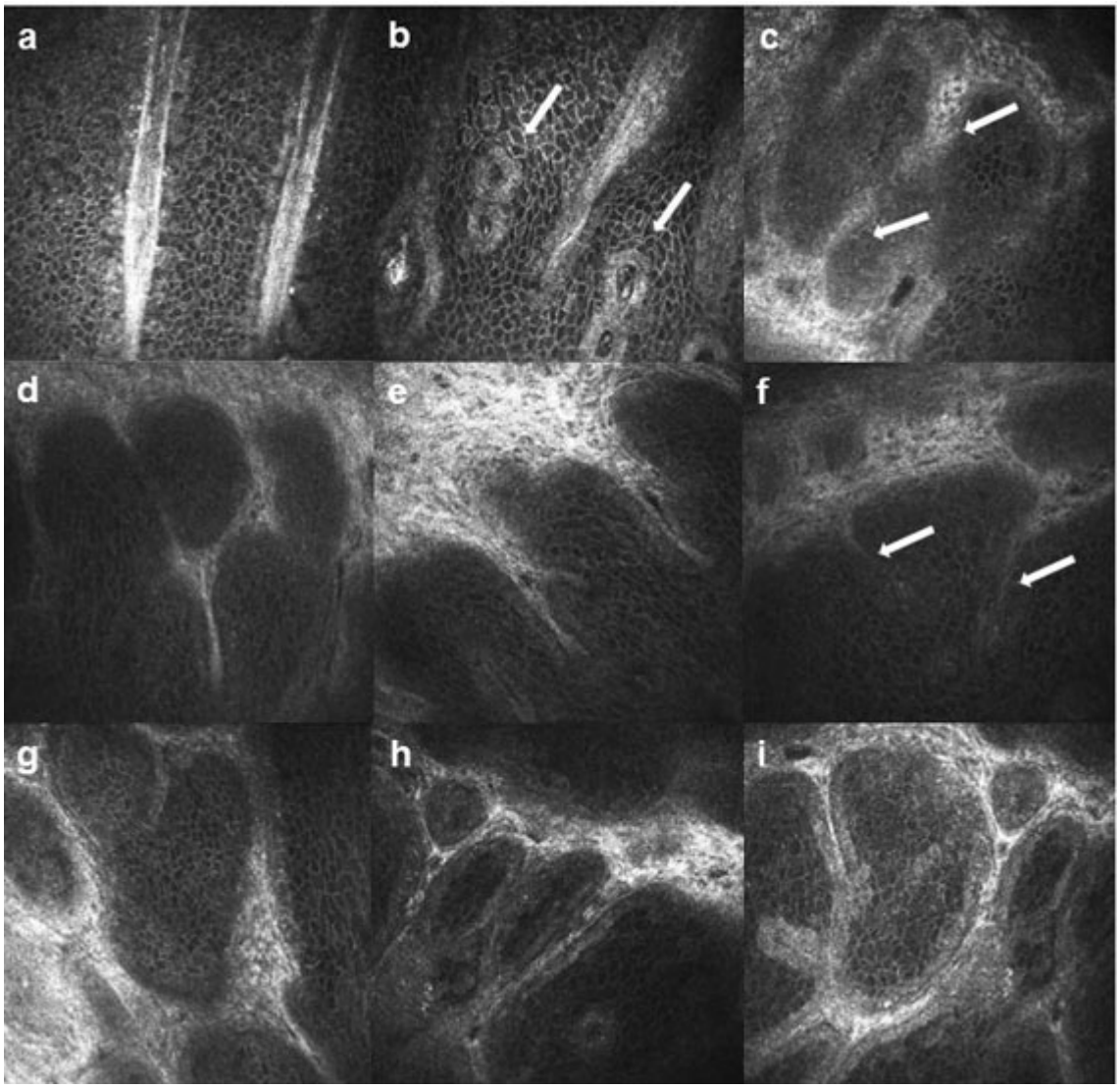

Fig. 2. **IVCM image of the superior limbus.**

a — "classic" form of POV in the form of hyperreflective double-contoured linear structures; b — presence of FSP among progenitor structures of the superior limbus (arrows); c–i — variants of atypical forms of POV: c — short shallow indistinct palisade-like structures united by horizontal crosspieces (arrows); d — honeycomb-like structure of POV organization; e — short shallow stubs of POV with a bifurcation at the end; f — hyperreflective formations connecting barely noticeable palisade-like structures (arrows); g, h — the honeycomb structure of POV, with trabecular stubs at the end; i — limbal crypts presented in the form of circular formations.

high sensitivity of this diagnostic method. An extrapolation of the tomography data in multiple overlapping IVCM images allowed visualizing the same structure and shape of the POV in identical areas as well as the location of the FSP.

By comparing the abilities of LSCM and AS-OCT to visualize POV, a strong positive correlation (r_S = 0.99, p<0.05) was revealed between the results obtained in both the superior and inferior limbus. The altered structure of POV as truncated, short limbal crypts, palisade deformation in the form of unstructured hyperreflective formations hampered their visualization by OCT and did not allow speaking to the presence of limbal progenitor structures only in one of the 30 examined eyes.

Discussion

In clinical practice, knowledge about the presence or absence of POV is an important criterion for preservation of the LSC, ensuring the regeneration and renewal of the cornea. A dysfunction in the limbal epithelium, manifested by abnormal conjunctival-corneal regeneration, significantly worsens the visual prognosis and quality of life among patients. However, the absence of palisades is not an absolute criterion of limbal deficiency. It is known that in 10-20% of individuals without apparent pathology of the cornea, POV are not visualized, especially in persons with weak pigmentation of skin and elderly patients [5, 9, 10]. In the work of D. Patel et al., all 16% of patients

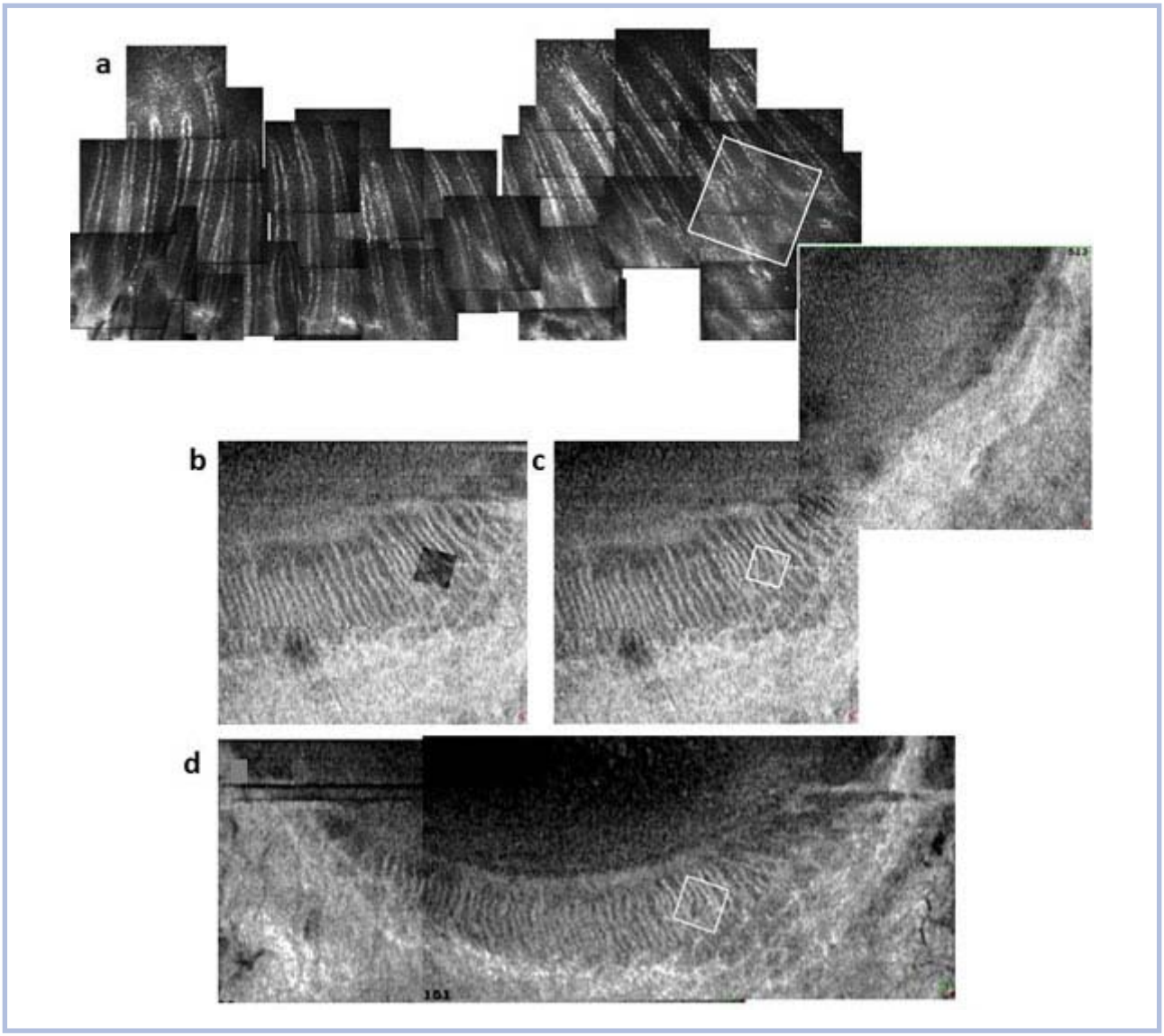

Fig. 3. **The results of the study of the inferior limbus of patient A., 46 years old.**

a — multiple IVCM image: well-defined POV arranged in the form of a pile fence with hyperreflective limbal basal cells; b, c, d — OCT images of an identical area of the limbus performed via 3D Cornea protocol (En Face imaging), a similar pattern of POV is highlighted by a white border. A gradual decrease in the height of the POV to the point of impossibility of their rendering in the horizontal meridian of the cornea is observed; b — IVCM image put onto the relevant area of an OCT image; c — AS-OCT was performed on the date of patient examination; d — OCT image performed in an identical area one week after the first visit.

with missing inferior limbus palisades were of the older age group (57 years and older) [9]. According to T. Zheng, a visualization of the inferior POV was possible only in 40% of individuals older than 60 years [10]. In this study, much like in those of other authors [14], limbal progenitor structures according to IVCM were found in all subjects, whose maximum age did not exceed 56 years.

The description of limbus progenitor structures in our work is not inconsistent with the data obtained earlier by other authors [9, 12, 14], but it gives a more precise characterization of the structural features of limbal patterns in the superior hemisphere of the cornea. According to the gradation proposed by W. Townsend in 1991, different variants of POV organization are possible: as standard, enhanced and diminished patterns [5]. In our work, we saw a standard "classic" phenotype of POV in the form of parallel lines in the inferior limbus, while the diminished limbal trabeculae stretched in the vertical meridian, localized mainly in the superior hemisphere of the cornea that corresponds to the data given by W. Townsend [5]. A linear and bifurcated structure of POV cornea is also comparable with clinical observations [4, 9] and with the data of histological studies on cadaver eyes [17].

Currently, the reasons for the formation of the so-called "tracks" and "streaks", extending from the apical end of POV to the center and interrupting the regular mosaic of basal cells remain uncertain in the IVCM pattern of the limbus area. These structures were described previously [9, 14] and, according to A. Miri, are the undulations in the basal membrane and underlying stroma.

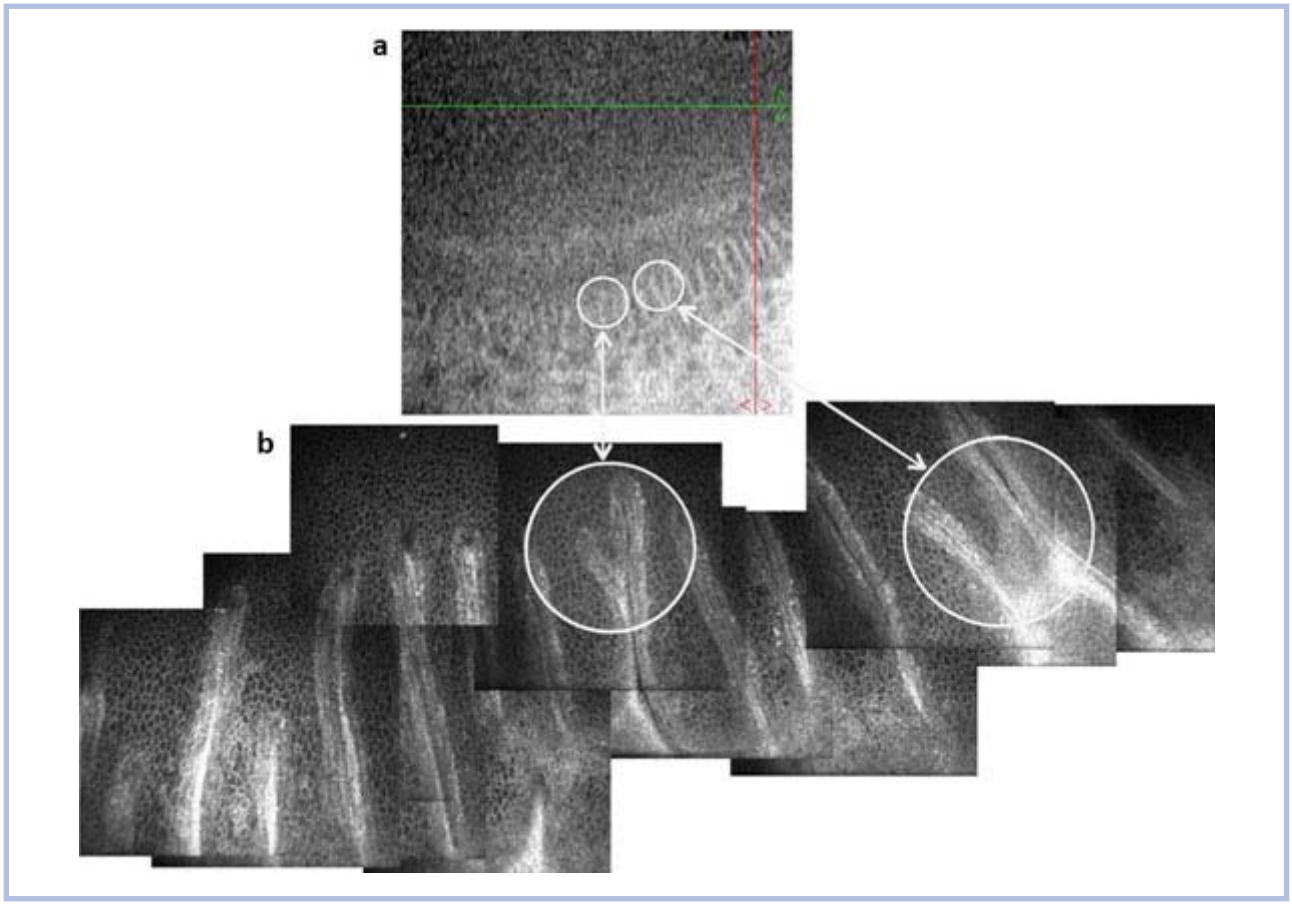

Fig. 4. **The results of the examination of the inferior limbus of patient S., 27 years old.**

a — AS-OCT image (3D Cornea protocol, En Face mode, the image size is 4x4 mm); b — multifield IVCM image of the identical area of the limbus: POV of the same shape are visualized; the identical areas being marked with white circles.

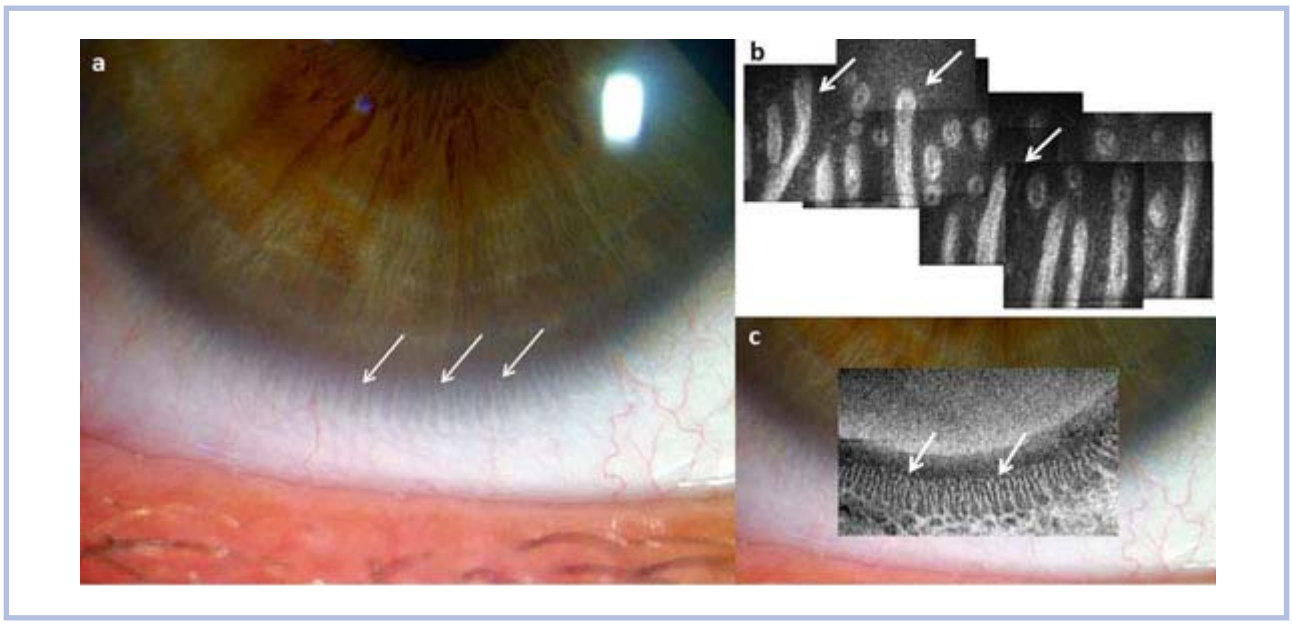

Fig. 5. **The results of the examination of the limbus of patient Sh., 35 years old.**

a — colored photo of the inferior limbus of the cornea: POV are visualized in the form of light trabeculae oriented to the center of the cornea (arrows); b — multifield image of the limbus according to IVCM data: POV (arrows) and multiple FSP are visualized; c — AS-OCT image put onto the relevant area of an image of the limbus of the cornea: AS-OCT image clearly shows POV (arrows) and multiple FSP comparable to IVCM data.

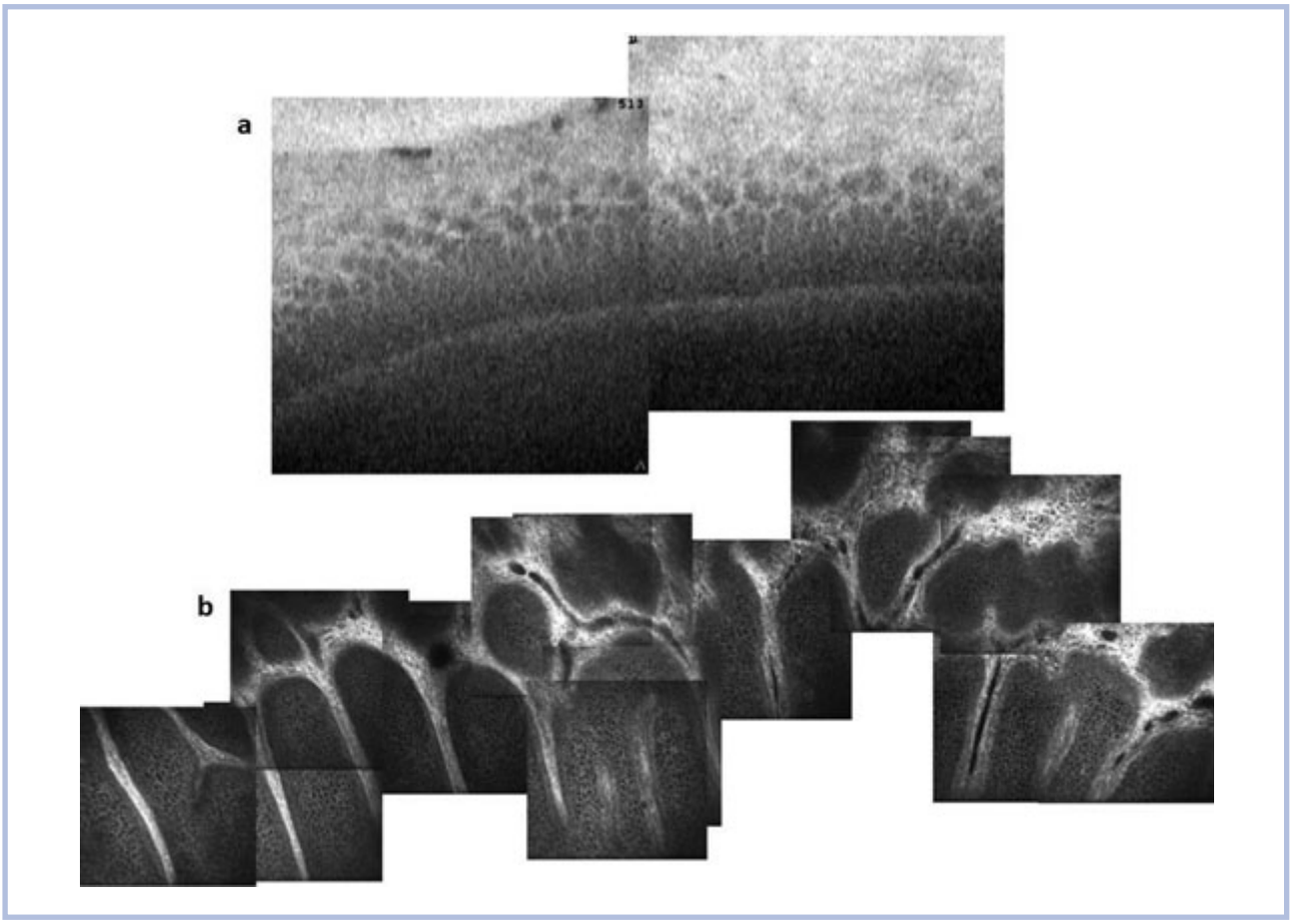

Fig. 6. **The results of the examination of the superior limbus of patient K., 25 years old.**

a — double AS-OCT image in which the honeycomb structure of POV with trabecular stubs at the end is clearly visible; b — multifield IVCM image of the identical area of the limbus: POV repeating the pattern seen in the AS-OCT images.

The dark areas correspond to the areas where no cells would be present. The appearance of such dark areas, according to the authors [18], is caused by folds of connective tissue under the germ cells. The altered topography of the basal membrane and its uneven surface facilitate the fixation of the epithelial layer and increase its resistance to traumatic factors [18]. In addition, similar dark curvilinear columns have been proposed as a feature of corneal membrane dystrophy [18]. However, the data of IVCM epithelial basement membrane dystrophy (map-dot-fingerprint dystrophy), which is characterized by an excessive growth and folding of the basal lamina, are different from the above descriptions. The folds of the abnormal basal membrane in this pathology are visualized as linear hyperreflective structures insinuated into the corneal epithelium, in contrast to the dark hyperreflective areas with winding contours observed in normal healthy individuals [19]. The analysis of the scans of dark curvilinear columns ("streaks") revealed the presence of basal epithelial cells contrasting with the adjacent hyperreflective cells. The nature of radially directed dark "tracks" ("streaks") was described by W. Townsend in detail [5]. He connects the appearance of dark "streams" with the centripetal movement of epithelial basal cells from the limbus to the center of the intact cornea. A set of dark streaks running from the periphery to the center, imitates the vortex, spoke-wheel or whirlpool patterns. This ability to migrate that the basal cells of the limbus show is required to maintain the pool of cells of the corneal epithelium and its self-renewal.

Our analysis of the literature revealed no articles that matched the results of POV visualization with the IVCM and AS-OCT (En Face) methods *in vivo*. The existing works have analyzed the image of POV obtained by these diagnostic techniques on cadaver eyes [15, 20].

The revealed advantages of IVCM included its high resolution that enabled to visualize the structure of the palisades at the cellular level. The main drawback of the methodology was the invasiveness of the study, limiting its use in patients with diseases of the corneal surface. In turn, the AS-OCT of the limbus zone did not require contact with the cornea, also had a high resolution, high speed and scanning area up to 4*8 mm, and was easily endured by subjects. The image obtained by OCT allowed one to analyze the structure and the density of the POV in the superior or inferior hemispheres of the cornea

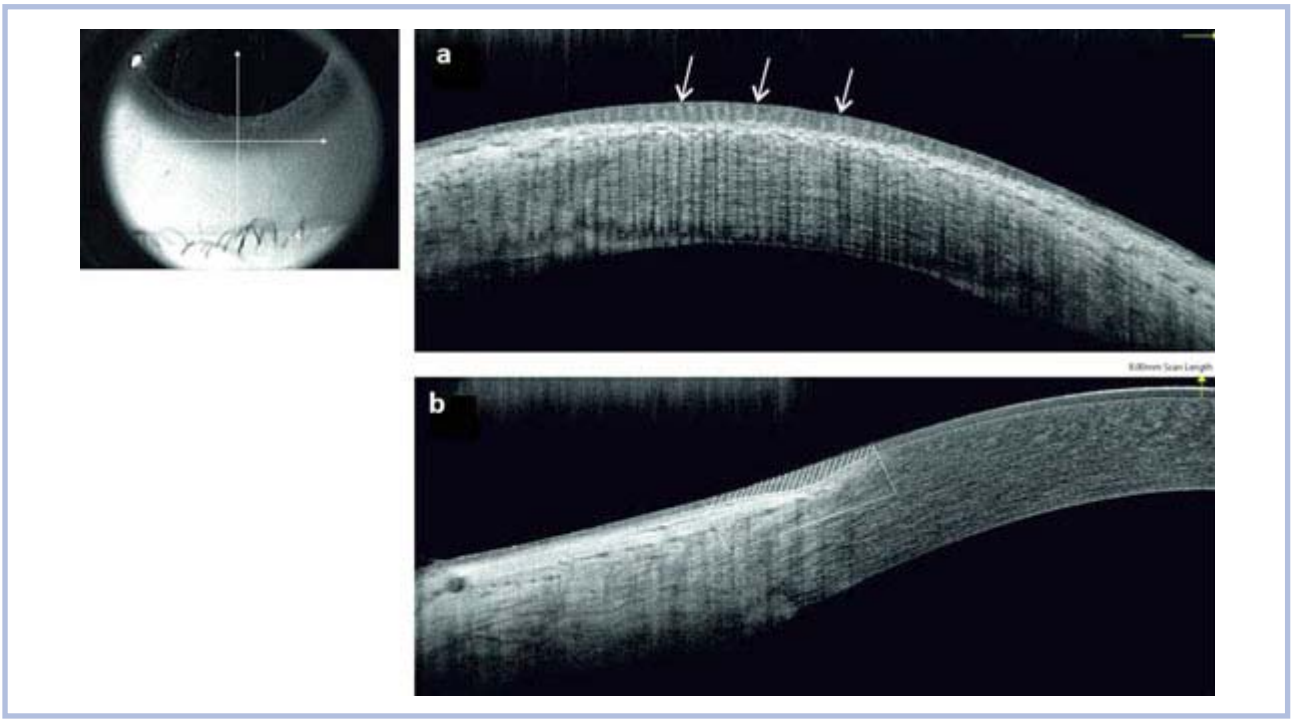

Fig. 7. **AS-OCT of the inferior limbus according to the Cornea Cross Line protocol.**

a — trabeculae in the form of oblong hyperreflective formations are defined on the horizontal scan (arrows); b — bed of the POV is visualized as a characteristic deepening of the sclera at the site of its corneoscleral transitional zone (this area is shaded) on the vertical scan which is perpendicular to the limbus.

as well as visualizing the shape and length of the limbal crypts in one picture. An assessment of the consistency of the results of the diagnosis of limbal palisades performed by IVCM and AS-OCT revealed the presence of a strong positive relationship ($r_S = 0{,}99$, $p < 0.05$) in the visualization of limbal progenitor structures, which confirms the high degree of identity of the obtained images.

Thus, AS-OCT in 3D Cornea Protocol (En Face), with its high information content, clarity, good repeatability and reproducibility of the results can be considered as an alternative method in POV diagnostics.

Conclusion

AS-OCT data allows visualizing the structure of POV in detail and highly correlates with the results of IVCM. Considering the noninvasiveness, AS-OCT may be recommended as a way to determine the integrity of limbal progenitor structures and to choose type of treatment of corneal diseases associated with a deficiency of the LSC.

None declared.

REFERENCES

1. Vogt A. *Atlas of the Slitlamp-Microscopy of the Living Eye*. Berlin: Springer-Verlag; 1921:23.
2. Davanager M, Evensen A. Role of the pericorneal papillary structure in renewal of corneal epithelium. *Nature*. 1971;229:560-1.
3. Polisetty N, Fatima A, Madhira SL et al. Mesenchymal cells from limbal stroma of human eye. *Mol Vis*. 2008;14:431–42.
4. Goldberg MF, Bron AJ. Limbal palisades of Vogt. *Tran. Am Ophthalmol Soc*. 1982;80:155-71.
5. Townsend WM. The limbal palisades of Vogt. *Trans Am Ophthalmol Soc*. 1991;89:721-56.
6. Chi C, Trinkaus-Randall V, Delmonte DW. JCRS New insights in wound response and repair of epithelium. *J. Cell Physiol*. 2013;228(5):925-9. doi: 10.1002/jcp.24268.
7. Secker GA, Daniels JT. *Limbal epithelial stem cells of the cornea*. StemBook [Internet]. Cambridge (MA): Harvard Stem Cell Institute; 2008 -2009.
8. Takahashi N, Chikama T, Yanai R, Nishida T. Structures of the Corneal Limbus Detected by Laser-Scanning Confocal Biomicroscopy as Related to the Palisades of Vogt Detected by Slit-lamp Microscopy. *Jpn J Ophthalmol*. 2009;53:199–203. doi: 10.1007/s10384-008-0661-4.
9. Patel D, Sherwin T, McGhee C. Laser Scanning In Vivo Confocal Microscopy of the Normal Human Corneoscleral Limbus. *Invest Ophthalmol Vis Sci*. 2006;47:2823–2827. doi:10.1167/iovs.05-1492
10. Zheng T, Xu J. Age-related changes of human limbus on in vivo confocal microscopy. *Cornea*. 2008;27:782–786. doi: 10.1097/ICO.0b013e31816f5ec3.
11. Russell HC, Chadha V, Lockington D, Kemp EG. Topical mitomycin C chemotherapy in the management of ocular surface neoplasia: a 10-year review of treatment outcomes and complications. *Br J Ophthalmol*. 2010;94:1316–1321. doi: 10.1136/bjo.2009.176099.
12. Shortt AJ, Secker GA, Munro PM, Khaw PT, Tuft SJ, Daniels JT. Characterization of the limbal epithelial stem cell niche: novel imaging techniques permit in vivo observation and targeted biopsy of limbal epithelial stem cells. *Stem Cells*. 2007;25:1402-1409. doi: 10.1634/stemcells. 2006-0580

13. Li W, Hayashida Y, Chen Y, Tseng S. Niche regulation of corneal epithelial stem cells at the limbus. *Cell Res.* 2007;17(1):26-36. doi:10.1038/sj.cr.7310137.

14. Miri A, Al-Aqaba M, Otri AM, Fares U, Said DG, Faraj LA, Dua HS. In vivo confocal microscopic features of normal limbus. *Br J Ophthalmol.* 2012;96:530-536. doi:10.1136/bjophthalmol-2011-300550

15. Lathrop K, Gupta D, Kagemann L, Schuman J. Optical Coherence Tomography as a Rapid, Accurate, Noncontact Method of Visualizing the Palisades of Vogt. *Invest Ophthalmol Vis Sci.* 2012;53(3):1381-1387. doi: 10.1167/iovs.11-8524.

16. Lumbroso B, Huang D, Romano A, Rispoli M. Clinical en face OCT atlas. Jaypee-highlights; 2013:78-79.

17. Espana EM, Romano AC, Kawakita T, Pascuale M, Smiddy R, Tseng S. Novel enzymatic isolation of an entire viable human limbal epithelial sheet. Invest *Ophthalmol Vis Sci.* 2003;44:4275–4281.

18. Jester JV, Petroll WM, Feng W, Essepian J, Cavanagh HD. Radial keratotomy. 1. The wound healing process and measurement of incisional gape in two animal models using in vivo confocal microscopy. Invest Ophthalmol Vis Sci. 1992;33:3255-3270.

19. Guthoff R, Baudouin C, Stave J. *Atlas of Confocal Laser Scanning In-vivo Microscopy in Ophthalmology.* Berlin: Springer-Verlag; 2006: 51.

20. Sigal IA, Steele J, Drexler S, Lathrop KL, Identifying the Palisades of Vogt in Human Ex-vivo Tissue. *Ocular Surface* (2016). doi: 10.1016/j.jtos.2016.07.003.